

Angle-resolved photoemission investigation of the (2×1) carbidic carbon on Ni(110)

L. Papagno and M. Conti

Dipartimento di Matematica e Fisica, Università di Camerino, 62032 Camerino, Macerata, Italy

L. S. Caputi

Dipartimento di Fisica, Università della Calabria, 87036 Arcavacata di Rende, Cosenza, Italy

J. Anderson and G. J. Lapeyre

Department of Physics, Montana State University, Bozeman, Montana 59719

(Received 12 March 1990; revised manuscript received 13 February 1991)

Carbidic carbon on Ni(110) (2×1) C phase has been obtained by exposing the clean surface at 520 K to ethylene gas in the 10^{-7} -torr range. By angle-resolved photoemission experiments, bands of the carbon overlayer system have been mapped along the ΓX and ΓY directions of the surface Brillouin zone. The comparison of our data with photoemission measurements and theoretical calculations on similar systems suggests a possible carbon chemisorption on a threefold-coordination site at the (110) surface of nickel.

I. INTRODUCTION

The clean Ni(110) is an example of an unreconstructed surface and its structure, determined by low-energy electron diffraction^{1,2} (LEED) and Rutherford backscattering spectroscopy (RBS),³ consists of closely packed rows of atoms separated by troughs along the $\langle \bar{1}10 \rangle$ direction. The first two interlayer spacings are relaxed about -9% and $+3\%$, respectively, with respect to the bulk values. Adsorbate overlayers generally form a (2×1) superstructure and sometimes they induce a substrate reconstruction.⁴ This is the case, for instance, of hydrogen adsorbed at low temperatures, below 180 K.⁵⁻⁷

A carbon overlayer on Ni is an important system particularly because of its relevance to catalytic activity in the Fisher-Tropsch synthesis.⁸ The carbidic carbon, which is the active species for catalytic metanation in heterogeneous catalysis, can be deposited on the surface by cracking ethylene at 600 K.⁹ Indeed, several carbidic carbon overlayers on Ni single crystal have been investigated, for instance, on Ni(111) (Ref. 10) and Ni(100).¹¹⁻¹⁴ In the latter system carbon is known to induce a reconstruction of the top nickel surface layer, in which carbon atoms occupy the fourfold-hollow sites. In the former it is suggested that carbon occupies a threefold chemisorption site, so that each carbon atom is symmetrically coordinated to three nickel atoms as first neighbors. The suggested model is consistent with a theoretical calculation made by Feibelman^{15,16} for carbidic carbon on Ru(0001) and Rh(111): carbon atoms form tetrahedral s - p bonds with three neighboring substrate atoms, leaving a nonbonding p_z band partially filled at the Fermi level (FL) and the carbon $2p_{xy}$ band at 3.5 eV below FL.

Carbidic carbon on Ni(110) exhibits either a (4×5) or a (2×1) LEED pattern. It has been proposed that the carbidic overlayer in the (4×5) structure induces a substrate reconstruction so as to produce locally a square pyrami-

dal coordination of the carbon with the Ni atoms.¹⁷ The (2×1) structure formation seems to be favored by reacting ethylene at lower temperatures (~ 575 K) (Ref. 9) and up to now it has only been characterized by LEED.

In this work we report on angle-resolved photoemission experiments for the (2×1) carbidic phase on Ni(110) obtained by cracking ethylene at 520 K. The experimental two-dimensional band structure induced by carbidic carbon is presented and discussed in terms of possible chemisorption models.

II. EXPERIMENT

The experiments were performed at the University of Wisconsin Synchrotron Radiation Center with a SEY-ER-G monochromator using synchrotron radiation from the storage ring Aladdin. A double-pass angle-resolving cylindrical mirror analyzer (CMA) was used in the vacuum chamber whose pressure was in the 10^{-11} -torr range during photoemission experiments. The CMA was a commercial device which was retrofitted with an angle-resolving drum as in Knapp *et al.*¹⁸ The overall resolution ranged from 0.2 to 0.4 eV. The incidence angle of the light (p -polarized) θ_i was fixed at 45° .

Normal-emission photoemission data were obtained with the polarization vector \mathbf{A} lying in the $(\bar{1}10)$ plane of the nickel crystal. The out-of-normal-emission data were measured at an emission angle $\theta_e = 30^\circ$ with the electron spectrometer aperture in a plane almost perpendicular to the plane of incidence (and of polarization) of the light and containing the surface normal. In one set of measurements the emission plane was the (001) plane of the nickel crystal; in the second set the emission plane was the $(\bar{1}10)$ plane. The latter geometry was obtained with a 90° sample rotation which left all the rest unchanged (light and analyzer position).

The nickel sample, prepared in the standard way, was cleaned with argon-ion sputtering; the sample was held

with a thin foil of tantalum with a thermocouple in between. The sample was heated by a filament placed on its back, used as an electron gun. During sputtering the sample was kept at 570 K; this procedure permitted us to sputter away carbon atoms segregating to the surface. The sample was also periodically annealed at high temperatures (~ 1000 K). Many cycles of cleaning were needed to avoid carbon segregation to the surface due to the annealing temperature. Carbodic carbon was obtained by exposing the clean surface at 520 K to ethylene gas at a pressure around 10^{-7} torr. Auger spectroscopy showed that only a carbidiclike phase was present on the surface, whereas LEED changed from a (1×1) to a (2×1) structure after carbodic carbon deposition. We noticed, however, that a very clear and sharp (2×1) structure was not observable: in some cases very feeble extra spots were present. Further annealing of the (2×1) phase did not change the Auger spectrum or the LEED pattern up to 750 K, when carbodic carbon converts into graphitic carbon. The LEED pattern for the new phase assumed the (1×1) structure with presence of increased background.

III. RESULTS AND DISCUSSION

By monitoring the carbodic carbon Auger signal variation versus ethylene dose we observed that a saturation signal was reached after 60 langmuirs ($1 \text{ L} = 10^{-6}$

torr sec) at which value the LEED pattern assumed the (2×1) structure. According to the LEED pattern and Auger measurements we deduced, for this phase, a carbodic carbon coverage $\Theta = 0.5$ monolayers (ML).

Some normal-emission photoemission spectra, taken at different photon energies, are reported in Fig. 1. Carbodic carbon signals on Ni(110) and clean Ni(110) have been normalized to the emission of secondary electrons. Two clear peaks are visible in the original carbodic spectrum and in its difference (dashed line): one at about 1 eV, the second (more structured) centered at around 4.5 eV. The lack of any dispersion of these structures for varying photon energy suggests that the peaks are coming from induced two-dimensional carbodic carbon overlayer at Γ .

Some angle-resolved photoemission spectra taken along the $[\bar{1}10]$ direction at a collection angle $\theta_e = 30^\circ$ are reported in Fig. 2. As for the normal photoemission spectra, carbon-induced features are clearly visible but better visualized in the difference spectra. In Fig. 3 we display the experimentally derived bands along the ΓX symmetry line deduced from spectra recorded for 17–34-eV photon energy. We tentatively plotted the weak structure at 1 eV observed only for some photon energies, although such a structure could be a spurious peak coming from the subtraction procedure. In the figure is also indicated, at midway, the first surface Brillouin zone of the (2×1) structure, which corresponds to 0.63 \AA^{-1} . All data have been measured for k parallel

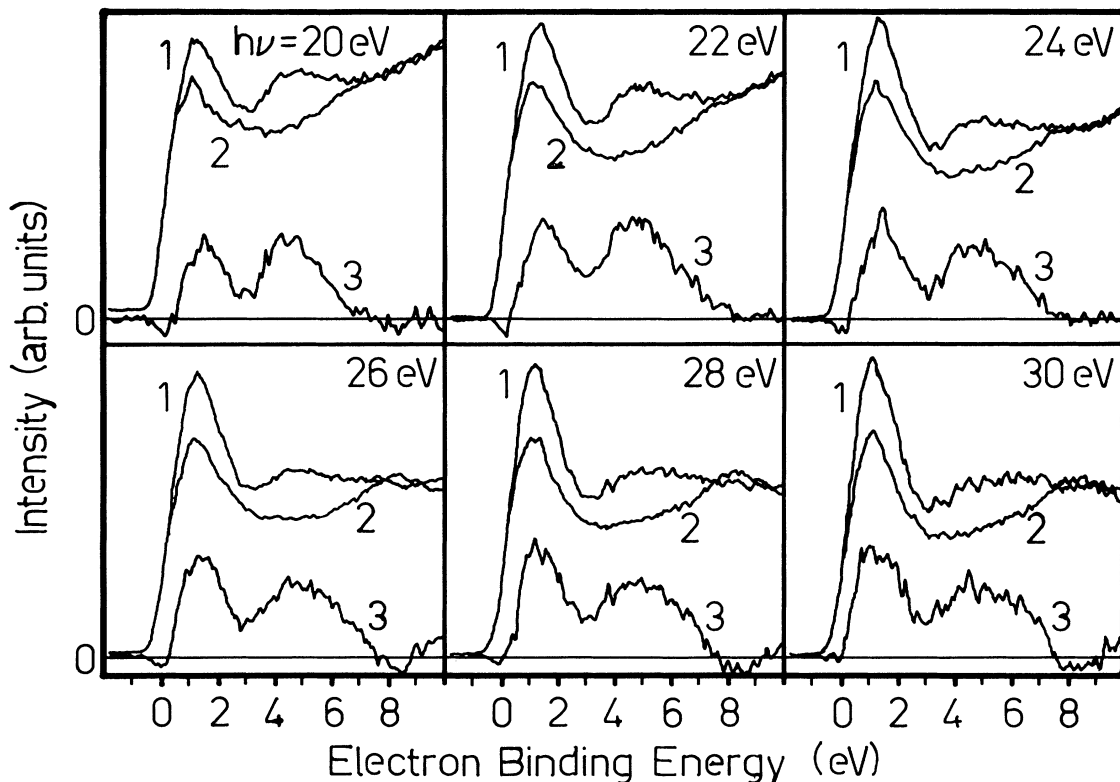


FIG. 1. Normal-emission photoemission energy distribution spectra recorded at various photon energies with the A vector in the $(\bar{1}10)$ plane from carbodic carbon (curve 1) and clean nickel (curve 2). Curve 3 is the difference spectrum between carbodic and clean nickel spectra.

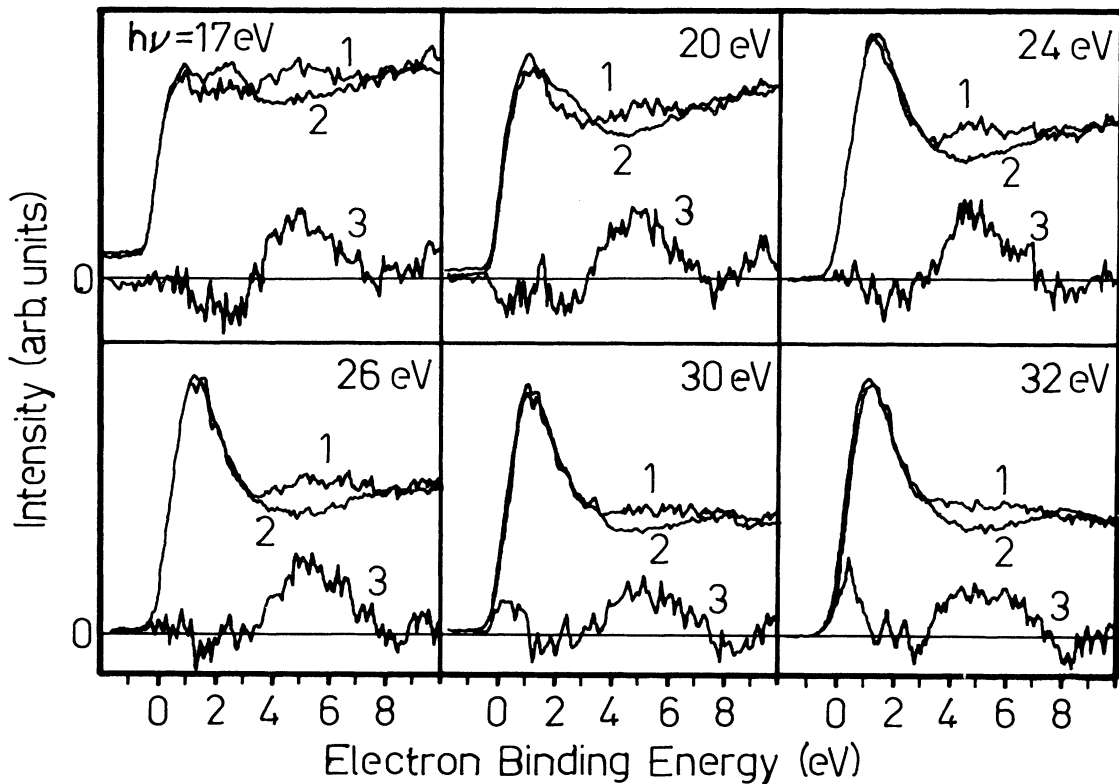


FIG. 2. Photoemission energy distribution spectra recorded at various photon energies at an emission angle $\theta_e = 30^\circ$ in the ΓX azimuth with the \mathbf{A} vector in the $(\bar{1}10)$ plane from carbidic carbon (curve 1) and clean nickel (curve 2). Curve 3 is the difference spectrum between carbidic and clean nickel spectra.

greater than 0.63 \AA^{-1} (solid bars) and backfolded to the first Brillouin (2×1) zone (thin bars). The bar's length qualitatively represents the peak width in the photoemission spectra; for instance, long bars mean that no other clear structure is detectable in the main broad peak,

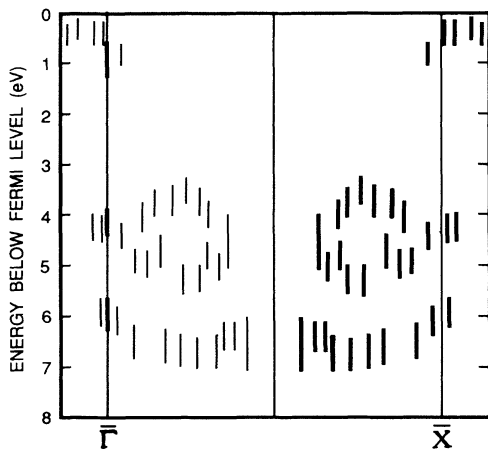


FIG. 3. An experimentally derived band structure along the ΓX symmetry line. The vertical line at midway (0.63 \AA^{-1}) indicates the first surface Brillouin zone of the $(2 \times 1)C$ structure. Thick bars indicate where experimental photoemission peaks occur, while thin bars relate to the same peaks folded back to the first $(2 \times 1)C$ zone.

while the shorter bars only suggest the possibility that more structures may be present within the main peak. In Fig. 3 are also indicated data obtained at normal emission (solid bars at Γ). The peak at about 1 eV is only located at Γ , and is not visible for high \mathbf{k} parallel; the structures at 4 and 6 eV show some energy dispersion (≤ 1 eV).

Angle-resolved photoemission spectra along ΓY , the $[001]$ direction, were taken for limited values of photon energy. The experimentally derived band-structure data points along the ΓY symmetry line are limited to a restricted \mathbf{k} -space region (from 0.6 to 0.9 \AA^{-1} with respect to 0.89 \AA^{-1} ΓY extension). We obtain a dramatic decrease of carbon-induced features in the 4–6-eV range and a systematic negative dip in the Ni $3d$ band region just below the FL. Figure 4 shows a typical set of spectra which illustrate this effect.

In Ref. 13 McConville *et al.* have studied experimentally and theoretically the electronic structure of the $(2 \times 2)C$ carbidic phase on Ni(110). The computed bidimensional band structure assumes that carbon atoms occupy the fourfold-hollow sites with a spacing of 0.58 \AA between the C layer and the top Ni layer. The main experimental result is that the C- $2p$ induced feature at 4 eV at Γ , dispersing down to 6 eV in their angle-resolved photoemission experiments, nicely reproduces the theoretical model. At normal emission only a shoulder at 4 eV is visible, while the peak at about 1 eV is sampled only at a 40° emission angle at 37-eV photon energy. Furthermore,

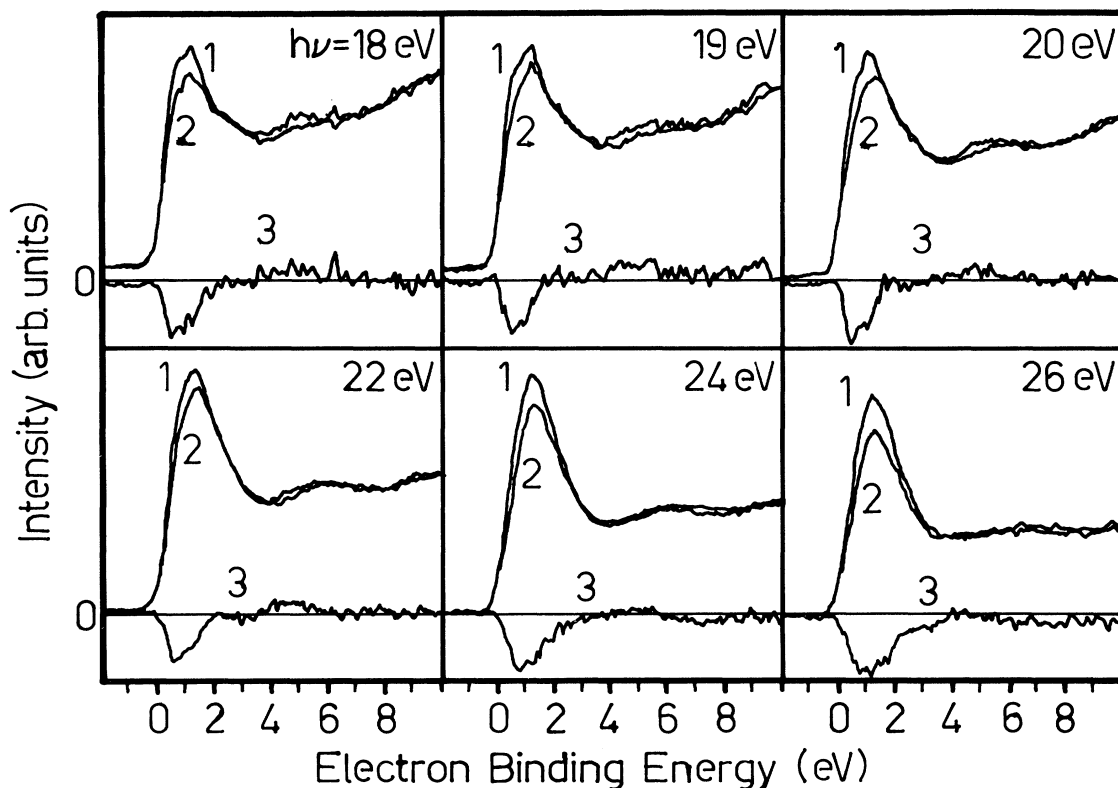


FIG. 4. Photoemission energy distribution spectra recorded at various photon energies at an emission angle $\theta_e = 30^\circ$ in the ΓY azimuth with the A vector in the (001) plane from carbidic carbon (curve 1) and clean nickel (curve 2). Curve 3 is the difference spectrum between carbidic and clean nickel spectra.

the increase observed in the Ni- d band over much of the surface Brillouin zone, not present in their model calculation, together with the observation that carbon strongly suppresses a clean Ni surface state, is interpreted in terms of reconstruction of the top nickel surface layer. Such a reconstruction implies a rotation of the groups of Ni atoms surrounding the fourfold-hollow adsorption sites. In our case we *do* observe a substrate feature suppression, but only along the ΓY direction—probably one of the clean nickel surface states along the ΓY symmetry line calculated by Dempsey, Grise, and Kleinman¹⁹—while a strong increase in the d -band region, on depositing a carbidic carbon layer, is observed but only in a very short range around Γ . The 1-eV feature is also clearly apparent in our integrated photoemission spectrum, together with the broad peak at around 5 eV (Fig. 5).

If we compare our spectrum in Fig. 5 with that of Rosei *et al.*¹⁰ obtained in their integral photoemission experiment for carbidic carbon on Ni(111), we see that the two spectra are very similar: they distinguish features at 1, 4.2, and a shoulder at 6.5 eV. The results of Ref. 10 are interpreted in terms of Feibelman's calculation for carbon overlayer on Ru(0001) (Ref. 15) and Rh(111) (Ref. 16) surfaces. One result of Feibelman's theoretical work is that Ru and Rh closely packed surfaces are shown to behave similarly for carbidic overlayer, and thus the

closely packed Ni(111) surface is expected to show strong similarities with them. On these metal surfaces carbidic carbon forms tetrahedral s - p bonding with its three neighboring substrate atoms. The carbon-carbon distance for this configuration is 2.49 Å, equal to the Ni

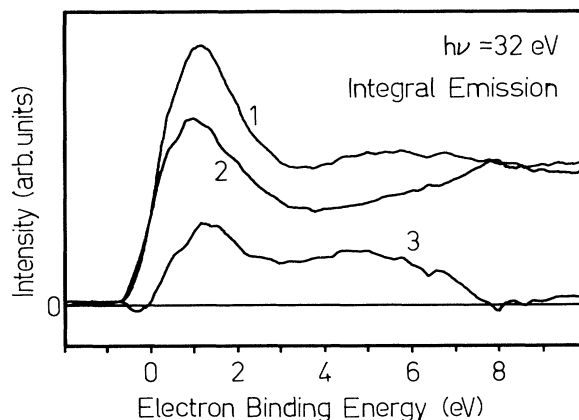


FIG. 5. Integral photoemission spectra recorded at 32-eV photon energy from carbidic carbon (curve 1) and clean nickel (curve 2). Curve 3 is the difference spectrum between carbidic and clean nickel spectra.

nearest-neighbors distance, too far apart for p_z orbitals to overlap in a π bonding. Thus the carbon $2p_z$ orbital is partially filled and has a peak in the density of states at the FL. The calculation also predicts a rather flat p_z band at 6.5 eV below FL at Γ , becoming a p_{xy} band going further into the surface Brillouin zone, together with another p_{xy} state located at 3.5 eV below FL.

We cannot directly compare our angle-resolved photoemission results with a model calculation of a different system. Many similarities, however, can be noted: we observe two bands at 4.2 and 6 eV which show small dispersion along the ΓX direction, together with a state at 1 eV almost located at Γ . Because, in our experimental conditions, the \mathbf{A} vector forms an angle of about 45° with the surface normal, both p_z and p_{xy} initial states can be excited, so that we cannot distinguish the symmetry of the initial states but, following Feibelman's model, we can identify the latter peak as the nonbonding $C-2p_z$ and the former as the $C-2p_{xy}$ bonding bands, respectively.

From these observations one deduction is that the electronic structure of (2×1) carbidic phase on Ni(110) is very similar to the carbidic carbon on Ni(111). One possible configuration for carbon adsorption on Ni(110) which reproduces, at least locally, carbidic carbon on Ni(111), is represented in Fig. 6, in which carbon atoms adsorb on a (111) microfacet at the Ni(110) surface. As regards the work-function variation due to carbidic overlayers on closely packed surfaces, Feibelman^{15,16} finds an increase in the work function: for instance, for a carbon-metal layer spacing equal to 1.27 Å an increase of 0.6 eV in the work function is calculated; it becomes 0.1 eV for 1 Å spacing. In our experiment we obtain a systematic negative variation of the work function. It could mean that the carbon overlayer is at an even lesser spacing than 1 Å with the first layer of the Ni atoms. This is exactly what one could expect if carbidic carbon partially sinks into the troughs along the $[\bar{1}10]$ direction, as suggested in the Fig. 6 model of our Ni(110) sample. This model is also supported by some preliminary results coming from a structural study that some of the authors have been carrying out on the same system.²⁰ The electron-energy-loss fine-structure (EELFS) technique,²¹ similarly to extended x-ray-absorption fine structure (EXAFS), extracts the radial distribution of neighbor atoms around the absorbing atom. By studying the EXAFS-like oscillations after the C-1s and Ni- M_{23} core level excitations, the following results have been obtained: (a) the carbon-nickel distance is 1.85 ± 0.05 Å; (b) the Ni first interlayer distance relaxes towards bulk distance after carbon deposition; and (c) a

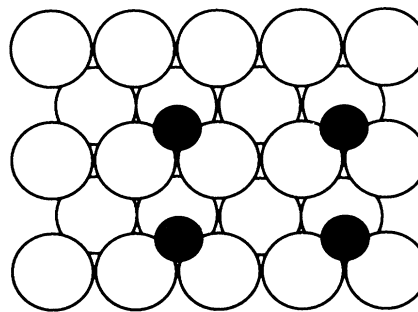


FIG. 6. Top view of the chemisorption model for carbidic carbon on Ni(110).

model calculation strongly favors the threefold chemisorption geometry of carbon on Ni(110) with respect to on-top or short- and long-bridge sites.

The carbon-nickel spacing of 1.85 ± 0.05 Å is, within the error bar, the same as that recently measured by surface EXAFS (Ref. 14) (SEXAFS) for the $(2 \times 2)C$ on Ni(100) system. Assuming as true the model at point (c) and the carbon-nickel distance equal to 1.85 Å, it emerges that the distance between carbon overlayer and the outermost nickel layer is ~ 0.45 Å, which is qualitatively in agreement with work-function measurements.

There is, however, another model which we used to fit our experimental data which, although less likely, cannot be totally excluded. This is the model proposed in Ref. 17 for $(4 \times 5)C$ on Ni(110), in which carbon induces a substrate reconstruction so as to form, locally, a square pyramidal coordination with four nickel atoms. However, this model is not consistent with our LEED pattern, which showed a (2×1) structure with some background. Paolucci *et al.*,¹⁷ on the other hand, did not succeed in obtaining a (2×1) LEED pattern for the same system. Probably more work is necessary to clarify this point, but a possible explanation could be that patches of both phases coexist; the amount of one with respect to the other could depend on details of sample preparation and carbon deposition.

ACKNOWLEDGMENT

We should like to thank the staff of the Synchrotron Radiation Center of Madison, Wisconsin, where this work has been carried out.

¹Mi. Xu and S. Y. Tong, Phys. Rev. B **31**, 6332 (1985).

²D. L. Adams, L. E. Peterson, and S. S. Sorensen, J. Phys. C **18**, 1753 (1985).

³R. Feidenhan's, J. Sorensen, and I. Stensgaard, Surf. Sci. **134**, 329 (1983).

⁴J. A. Stroscio, M. Paterson, and W. Ho, Phys. Rev. B **33**, 6758 (1986), and references therein.

⁵V. Panka, K. Christman, and G. Ertl, Surf. Sci. **136**, 307 (1984).

⁶K. Christman, V. Panka, R. J. Behm, F. Chehab, and G. Ertl,

Solid State Commun. **51**, 437 (1984).

⁷G. Kleinle, V. Panka, R. J. Behm, and G. Ertl, Phys. Rev. Lett. **58**, 148 (1987).

⁸R. D. Kelley and D. W. Goodman, in *The Chemical Physics of Solid Surfaces and Heterogeneous Catalysis*, edited by D. A. King and D. P. Woodruff (Elsevier, Amsterdam, 1982), Vol. 4, p. 453; D. W. Goodman, R. D. Kelley, T. E. Madey, and J. T. Yates, Jr., J. Catal. **63**, 226 (1980).

⁹J. C. McCarty and R. J. Madix, Surf. Sci. **54**, 121 (1976).

- ¹⁰R. Rosei, S. Modesti, F. Sette, C. Quaresima, A. Savoia, and P. Perfetti, *Solid State Commun.* **46**, 871 (1983); *Phys. Rev. B* **29**, 3416 (1984).
- ¹¹J. H. Onuferko, D. P. Woodruff, and D. W. Holland, *Surf. Sci.* **87**, 357 (1978).
- ¹²L. S. Caputi, G. Chiarello, and L. Papagno, *Surf. Sci.* **162**, 259 (1985).
- ¹³F. C. McConville, D. P. Woodruff, S. D. Kevan, M. Weinert, and J. W. Davenport, *Phys. Rev. B* **34**, 2199 (1986).
- ¹⁴M. Bader, C. Ocal, B. Hillert, J. Haase, and A. M. Bradshaw, *Phys. Rev. B* **35**, 5900 (1987).
- ¹⁵P. J. Feibelman, *Surf. Sci.* **103**, L149 (1981).
- ¹⁶P. J. Feibelman, *Phys. Rev. B* **26**, 5347 (1982).
- ¹⁷G. Paolucci, R. Rosei, K. C. Prince, and A. M. Bradshaw, *Appl. Surf. Sci.* **22/23**, 562 (1985).
- ¹⁸J. A. Knapp, G. J. Lapeyre, K. V. Smith, and M. M. Traum, *Rev. Sci. Instrum.* **53**, 781 (1982).
- ¹⁹D. G. Dempsey, W. R. Grise, and L. Kleinman, *Phys. Rev. B* **18**, 1270 (1979).
- ²⁰L. S. Caputi, R. Tucci, A. Amoddeo, and L. Papagno, *Phys. Rev. B* (to be published); A. Amoddeo, L. S. Caputi, R. Tucci, and E. Colavita (unpublished).
- ²¹L. Papagno, M. De Crescenzi, G. Chiarello, E. Colavita, R. Scarmozzino, L. S. Caputi, and R. Rosei, *Surf. Sci.* **117**, 525 (1982); M. De Crescenzi, L. Papagno, G. Chiarello, R. Scarmozzino, E. Colavita, R. Rosei, and S. Mobilio, *Solid State Commun.* **40**, 613 (1981).